RESEARCH

Establishment and validation of nomograms for predicting mesorectal lymph node staging and restaging

Zixuan Zhuang[1] · Xueqin Ma[2] · Yang Zhang[1] · Xuyang Yang[1] · Mingtian Wei[1] · Xiangbing Deng[1] · Ziqiang Wang[1]

Abstract

Background Preoperative determination of lymph node (LN) status is crucial in treatment planning for rectal cancer. This study prospectively evaluated the risk factors for lymph node metastasis (LNM) at staging and restaging based on a node-by-node pairing between MRI imaging findings and histopathology and constructed nomograms to evaluate its diagnostic value.

Methods From July 2021 to July 2022, patients with histopathologically verified rectal cancer who underwent MRI before surgery were prospectively enrolled. Histological examination of each LN status in the surgical specimens and anatomical matching with preoperative imaging. Taking histopathological results as the gold standard, federating clinical features from patients and LN imaging features on MRI-T2WI. Risk factors for LN metastasis were identified by multivariate logistic regression analysis and used to create a nomogram. The performance of the nomograms was assessed with calibration plots and bootstrapped-concordance index and validated using validation cohorts.

Results A total of 500 target LNs in 120 patients were successfully matched with node-by-node comparisons. A total of 353 LNs did not receive neoadjuvant therapy and 147 LNs received neoadjuvant chemoradiotherapy (neoCRT). Characterization of LNs not receiving neoadjuvant therapy and multivariate regression showed that the short diameter, preoperative CEA level, mrT-stage, border contour, and signal intensity were associated with a high risk of LN metastasis ($P < 0.05$). The nomogram predicted that the area under the curve was 0.855 (95% CI, 0.794–0.916) and 0.854 (95% CI, 0.727–0.980) in the training and validation cohorts, respectively. In the neoadjuvant therapy group, short diameter, ymrT-stage, internal signal, and MRI-EMVI were associated with LN positivity ($P < 0.05$), and the area under the curves using the nomogram was 0.912 (95% CI, 0.856–0.968) and 0.915 (95% CI, 0.817–1.000) in two cohorts. The calibration curves demonstrate good agreement between the predicted and actual probabilities for both the training and validation cohorts.

Conclusion Our nomograms combined with preoperative clinical and imaging biomarkers have the potential to improve the prediction of nodal involvement, which can be used as an essential reference for preoperative N staging and restaging of rectal cancer.

Keywords Rectal cancer · Mesorectal lymph nodes · Nomogram · MRI · N-staging · Neoadjuvant therapy · Node by node · Restaging

Introduction

Rectal cancer is the third most common cancer worldwide and has high mortality and morbidity [1]. With the widespread application of multidisciplinary treatment strategies, the treatment of rectal cancer has improved, but due to the high incidence of recurrence and metastasis for patients with stage III and IV locally advanced rectal cancer (LARC), postoperative mortality remains high [2]. Numerous previous studies have shown that LNM is a major prognostic factor for overall survival in patients with rectal cancer. In clinical practice, LN involvement is assessed before treatment to guide personalized treatment. Therefore, the accurate assessment of the status of LNs is of great significance for the management and treatment strategies of rectal cancer [3, 4].

The initial diagnostic tools currently used for N staging, including magnetic resonance imaging (MRI) and computed tomography (CT), are widely used in clinical practice [5, 6].

✉ Ziqiang Wang
wangziqiang@scu.edu.cn

1 Department of General Surgery, Colorectal Cancer Center, West China Hospital, Sichuan University, Chengdu, China

2 Department of Radiology, The Second Affiliated Hospital of Chongqing Medical University, Chongqing, China

However, since no uniform standard for defining LN status imaging exists, the current means of predicting LNM is discouraging. Until now, it is still common to predict the N stage according to the size and morphology of the LN [7, 8]. But so far, due to the lack of pathological ground truth for each LN, most studies have evaluated LNM indirectly through whole specimen sampling. According to research, features at the LN level are more predictive than those at the tumor level [9–12].

In contrast, there is a greater debate over the accuracy of restaging after chemoradiotherapy (CRT), since neoadjuvant treatment alters the size, shape, and texture of positive LNs. For patients with LARC receiving neoadjuvant therapy, accurate N staging is critical when planning organ preservation therapy, as nonresected lymph node metastasis-positive can lead to local recurrence or distant metastasis [13–15]. All these contradictions have led to more precise clinical N staging.

Previous studies have found that the pT-stage, depth of submucosal invasion, extramural venous invasion, and poorly-differentiated adenocarcinoma were strongly associated with LNM [16, 17]. Nevertheless, most of these risk factors were based on postoperative pathological results, which may be inappropriate for preoperative staging and restaging.

As part of a prospective study for imaging accuracy in diagnosing mesorectal LN staging, this study used preoperative clinical and imaging biomarkers to construct nomograms of LNM based on a node-by-node comparison and comprehensively evaluated the diagnostic value.

Methods and materials

This methodological study was based on a prospective study for imaging accuracy in diagnosing mesorectal lymph node staging (ChiCTR2100052441). The Medical Ethics Committee of West China Hospital approved the study, and written informed consent was obtained from all patients before surgery.

Patients

From July 2021 to July 2022, 120 patients with histopathologically verified rectal cancer underwent radical surgery. The inclusion criteria were as follows: (1) rectal carcinoma located ≤ 10 cm above the anal verge; (2) radical surgery scheduled within 2 weeks after rectal MRI (including 6–8 weeks after the completed neoadjuvant treatment); (3) patients with $1 \leq LNs \leq 15$ on preoperative imaging findings. The exclusion criteria were as follows: (1) complete imaging and clinical data were unavailable.

Therapeutic regimen

Seventy-two patients underwent primary surgery without neoadjuvant therapy. Forty-eight patients received neoadjuvant chemoradiotherapy (neoCRT) and delayed surgery. Concurrent chemoradiotherapy regimen: concomitant radiation therapy (46 to 50.4 Gy/23 to 28 fractions, 5.5 to 6 weeks) and one to five cycles of simultaneous chemotherapy with capecitabine (865 mg/m2/bid).

MR imaging protocol

MR imaging was performed with a 3 T MAGNETOM Skyra MR scanner (Siemens Healthineers, Malvern, PA, USA) employing an 18-channel body coil. All patients were given an intravenous antiperistaltic agent (10 mg raniscopamine hydrochloride) 30 min before MRI for bowel preparation. The high-resolution rectal MRI protocol comprised turbo spin–echo sagittal, oblique coronal, oblique axial T2-, and diffusion-weighted imaging. The scan parameters used for the oblique axial T2-weighted imaging sequence were as follows: repetition time/echo time, 6890/100; slice thickness, 3 mm; voxel size, $0.3 \times 0.3 \times 3$ mm; field of view, 180 mm; matrix, 384×346; slices, 48; average, 3; total scanning time, 5 min, and 5 s; parallel acquisition technique with generalized autocalibrating partial parallel acquisition acceleration factor. The oblique axial DWI sequence was a transverse echo-planar imaging diffusion sequence with 1000 s/mm^2 as the highest b value. The same parameters, such as field of view (FOV), slice thickness, and gap, were used in DWI to match the tumor on the oblique axial T2WI. The total scan time was 30 min.

Radiologic–pathologic node-by-node comparison

All rectal MRI images of patients with rectal cancer were analyzed preoperatively by a radiologist with more than 15 years of experience interpreting rectal imaging studies. MRI high-resolution oblique-axis T2-weighted imaging and DW images were used as evaluation sequences. Similar to the method described in previous reports [18–20], after referencing DWI, the radiologist performed anatomic correlation matching with T2WI to confirm regional LNs and recorded the nodal size, nodal location, and level sequence of each LN. All LNs evaluated by imaging were drawn on anatomical maps to obtain accurate histology-imaging correlation node by node (Fig. 1). All patients underwent total mesorectal excision (TME) within 2 weeks of the imaging examination. Fresh specimens were pinned to a foam board, sent to the pathology laboratory for macroscopic examination, and then immersed in formalin saline for at least 72 h for fixation. A pathologist with 15 years of

experience guided each specimen by a 3 mm ruled template and sectioned at 3 mm intervals transversely, perpendicular to the long axis of the mesorectum, from the distal aspect to the proximal aspect. All slices were numbered and photographed. LNs were carefully identified on each slice, and the anatomical map was used as a template for node-by-node correspondence. All matched LNs were numbered and placed in individual trays for processing. In subsequent microscopy, all slides were stained with hematoxylin and eosin. The benign and malignant LNs were reported according to the microscopy results.

Clinical and imaging data collection

The clinical data included patient age, sex, carcinoembryonic antigen (CEA), and carbohydrate antigen 19–9 (CA19-9) levels. The histological grades were obtained from pathological reports.

In MRI data assessments, two radiologists experienced in reading rectal MRI were blinded to the histological information and independently reviewed the entire MR images. The mrT-stage, tumor diameter, depth of invasion, MRI-EMVI score, and MRI-CRM score were determined. The maximum short diameter (mm) of the target LNs was measured on axial T2-weighted imaging. In the neoadjuvant therapy group, the maximum short diameter (mm) of the residual LNs on the post-CRT MRI was measured and matched with the corresponding LNs on the pre-CRT MRI. Calculated the short diameter regression (mm) on the pre/post-CRT MRI and grouped it according to the degree of regression. LNs that disappeared on the post-CRT MRI were excluded. Referring to Kim et al. [8], the LN shape was divided into three categories: round, ovid, and others. The border contour of LN was divided into four categories: smooth, lobulated, spiculated, and indistinct. The internal signal of LN was divided into two types: homogeneity and heterogeneity. Signal intensities of LN were classified as high, iso, or low signal intensities compared to the primary tumor. The

intraclass correlation coefficients calculated for parameters initially extracted by the two radiologists ranged from 0.669 to 0.968, and then referred them for senior radiologist review to make the final judgment.

Statistical analysis

All analyses were performed using R version 3.6.1 (http://www.Rproject.org). The continuous variables were examined for normality (Kolmogorov–Smirnov test), data are presented as the mean $\pm$ standard deviation (SD) when a normal distribution was satisfied, and the independent-samples t-test was used for intergroup comparison. If the data did not correspond to a normal distribution, they are presented as medians (interquartile ranges, IQRs), and the Mann–Whitney rank-sum test was utilized for the different analyses of two groups. The chi-square test was used to compare categorical variables between groups. Risk factors with a P-value of < 0.05 in univariate analysis were included in multivariate analysis. Multivariate logistic regression analysis was performed to identify independent risk factors using backward stepwise selection. Nomograms were developed based on the multivariate logistic regression model. The performance of the nomogram was evaluated using the concordance index and calibration plot. The nomogram's sensitivity, specificity, and accuracy for LN metastasis were calculated. Receiver operating characteristic (ROC) curves and the area under the ROC curve (AUC) were used to assess the diagnostic value.

Results

From July 2021 to July 2022, a total of 120 cases were prospectively enrolled. Seventy-two patients did not receive neoadjuvant therapy, and forty-eight patients received neoadjuvant chemoradiotherapy. Table 1 summarizes and compares the basic
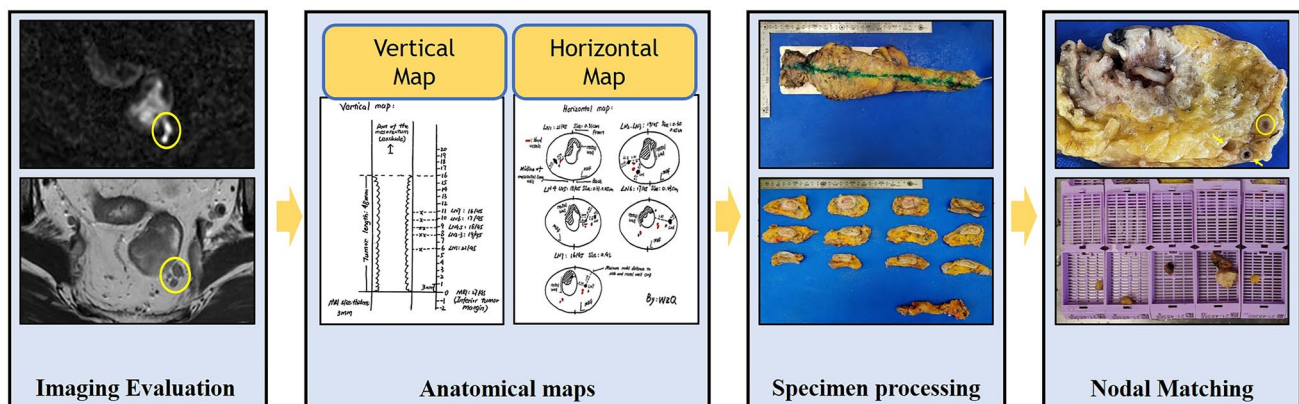

Fig. 1 Flow chart of node-by-node comparison of imaging with histopathology

Table 1 Characteristics of patients in the primary surgery and neoadjuvant therapy groups

Middle (5–10 cm)	39	14			13	15	
(y)mrT-stage			0.001*				0.016*
T1	5	0			4	1	
T2	23	0			12	2	
T3	25	16			12	16	
T4	1	2			0	1	
CA19-9 /(U·mL^{-1})			0.039*				0.393*
0–27	51	14			27	20	
> 27	3	4			1	0	
CEA/(ng·mL^{-1})			0.001*				0.658*
0–5	45	7			25	17	
> 5	7	11			3	3	
MRI-CRM			0.884*				0.018*
Positive	17	6			5	10	
Negative	37	12			23	10	
MRI-EMVI			0.078*				0.017*
Positive	10	7			3	8	
Negative	44	11			25	12	

PS primary surgery, *NT* neoadjuvant therapy, *(y)mrT-stage* (neoadjuvant therapy) mriT stage, *pN-* pathological benign lymph node, *pN+* pathological malignant lymph node, *CA19-9* carbohydrate antigen 19–9, *CEA* carcinoembryonic antigen, *CRM* circumferential resection margin, *EMVI* extramural vascular invasion

* chi-square test; ** rank-sum test

demographic characteristics, tumor characteristics, and clinical features of the neoadjuvant therapy/primary surgery groups and categorizes the two cohorts according to the (y)pN status.

For evaluation on a node-by-node basis, only those LNs that could be identified were included. A total of 532 LNs were identified during imaging evaluation. Of these, 500 were confirmed on histopathological findings. Conversely, only 500/1377 (36%) nodes harvested from the mesorectum on histopathological examination could be matched to nodes on imaging evaluation (Fig. 2). Among the 500 matched nodes, 353 did not receive neoadjuvant therapy. A total of 147 received neoadjuvant therapy. The 500 matched LNs were randomly allocated to a training cohort and a validation cohort in a ratio of 7:3.

Primary surgery group

Analysis of radiological features of 353 target LNs without neoadjuvant therapy, including 247 in the training and 106 in the validation cohort (Table 2).
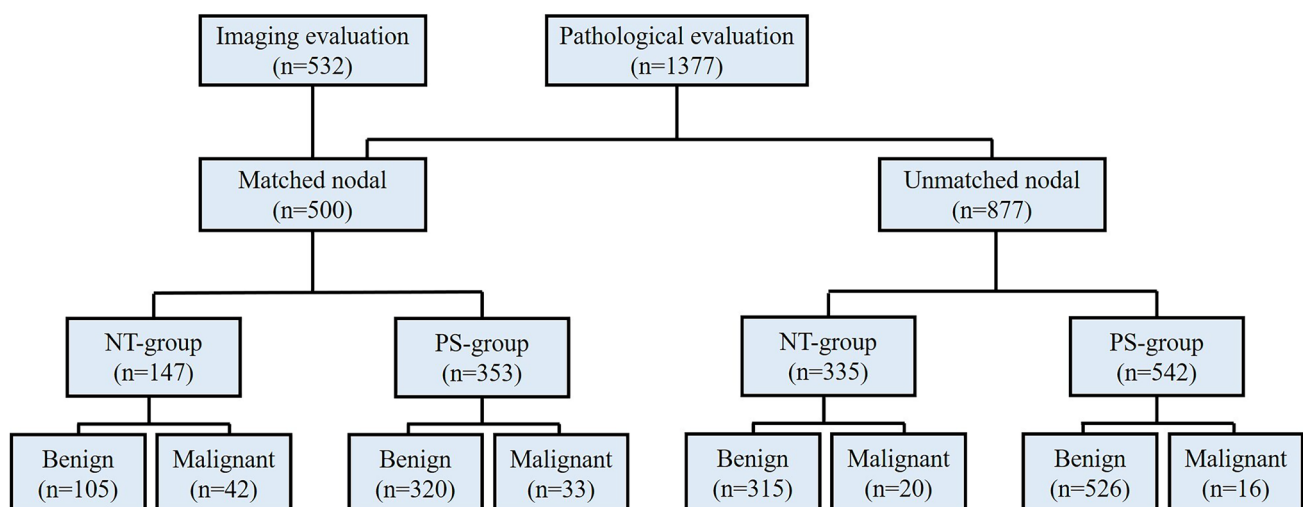

Fig. 2 Imaging characteristics versus the histologic findings in 1377 nodal of 120 patients

In both cohorts, the short diameter of positive was significantly greater than that of negative ($P < 0.001$). In the morphologic characterization, the shape, border contour, internal signal, and signal intensity were statistically different between the positive and negative LNs ($P < 0.05$). When the short diameter was 5.25 and 5.5 mm, the prediction of LN metastasis had a medium–low diagnostic ability. The short diameter yielded an AUC of 0.661 (95% CI, 0.520–0.802) and 0.749 (95% CI, 0.562–0.936) in the training and validation cohorts, respectively. The corresponding ROC curves and AUC values are shown in Fig. 3 and Table 3. The axial T2WI median short-axis diameters were 4.0 mm (range: 1.9–9.0 mm) and 5.6 mm (range: 1.6–11.8 mm) for the negative and positive nodules, respectively. The histogram of LN distribution under different short diameters is shown in Fig. 4.

The results of the multivariate analysis are shown in Table 4. Chosen the short diameter, shape, border contour, internal signal, signal intensity, mrT-stage, and preoperative CEA and CA19-9 level from the training cohort as covariates for logistic regression analysis. Multivariate

logistic regression results demonstrated that the short diameter, border contour, signal intensity, mrT-stage, and preoperative CEA level were independent predictors of LNM ($p < 0.05$). To quantitatively predict LN metastasis, a nomogram with 5 significant predictors is presented in Fig. 5. In the training cohort, the diagnostic accuracy of the nomogram was 75%, the AUC was 0.855 (95% CI, 0.794–0.916), and the sensitivity and specificity were 87 and 73.2%. Hosmer Lemeshow goodness of fit test $p = 0.917$. The C-index was 0.855 and was confirmed to be 0.828 via 1000 bootstrapping validation. The AUC of the nomogram was shown to be 0.854 (95% CI, 0.727–0.980) in the validation cohort (Fig. 3 and Table 3). The C-index was 0.932, and the bootstrapped-concordance index was 0.890. The calibration curves demonstrate good agreement between the predicted and actual probabilities for both the training and validation cohorts (Fig. 6).

The cranial-caudal distribution of the LN with the distal tumor margin is shown in Fig. 7. A total of 163/353 (46%) LNs were found at the level of the tumor; 98% (346/353) of LNs were seen at the level of the tumor or within 5 cm

Table 2 Lymph node characteristics in training and validation cohort in the primary surgery group

Feature	Training cohort ($n = 247$)		P-value	Validation cohort ($n = 106$)		P-value
	Malignant LN ($n = 23$)	Benign LN ($n = 224$)		Malignant LN ($n = 10$)	Benign LN ($n = 96$)	
Short diameter (mm)	5.26 (1.60–11.80)	4.07 (2.10–9.00)	0.001**	6.44 (3.10–8.20)	3.90 (1.90–7.60)	0.001**
Shape			0.344*			0.001*
Round	4	43		2	17	
Ovid	9	116		1	60	
Other	10	65		7	19	
Border contour			0.001*			0.009*
Smooth	2	84		0	40	
Lobulated	6	82		3	30	
Spiculated	10	25		5	13	
Indistinct	5	33		2	13	
Internal signal			0.006*			0.004*
Homogeneity	8	143		3	71	
Heterogeneity	15	81		7	25	
Signal						
Low	12	72	0.069*	5	25	0.212*
Iso	8	134		4	65	
High	3	18		1	6	
Distribution			0.509*			0.581*
Below the distal tumor	0	4		0	1	
Level of the tumor	14	102		3	44	
≤ 5 cm proximal to the tumor	9	116		7	51	
> 5 cm proximal to the tumor	0	2		0	0	

LN lymph node
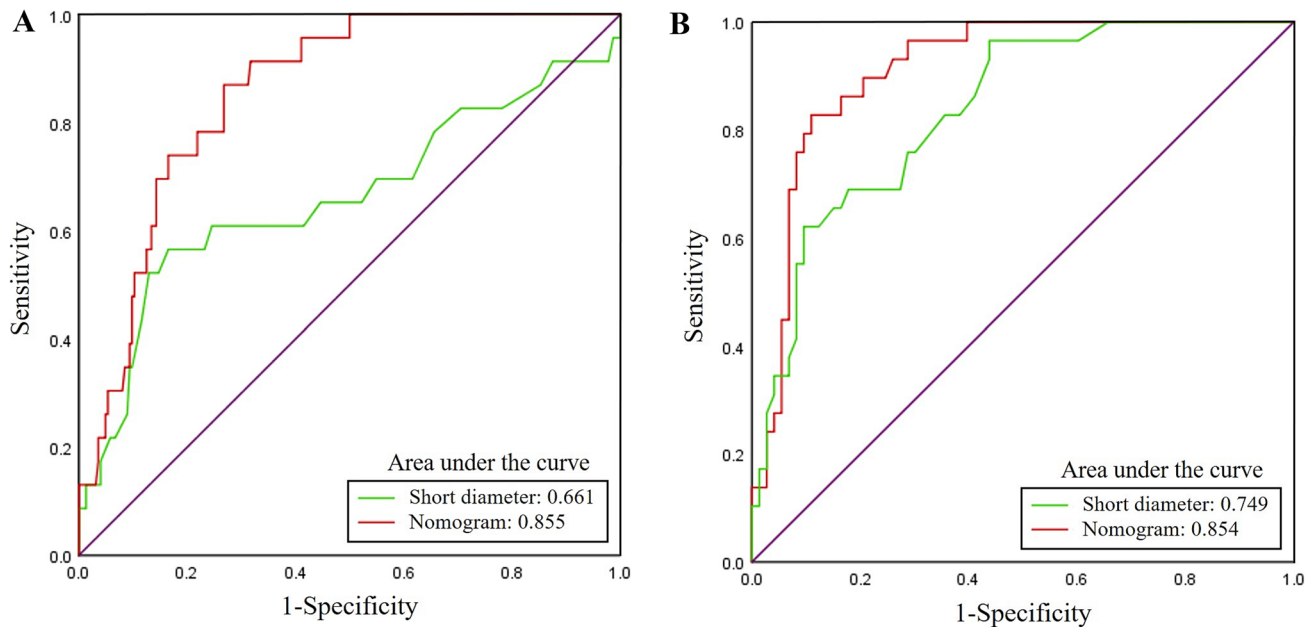
* chi-square test; ** rank-sum test

Fig. 3 Receiver operating characteristic (ROC) curve and prediction model based on short diameter and nomogram in primary surgery group. **A** ROC curve in the training cohort. **B** ROC curve in the validation cohort

proximal to the tumor. Five LNs were found below the distal tumor margin, and 2 LNs were found 5 cm beyond the proximal tumor. All positive LNs were distributed at the level of the tumor or within 5 cm proximal to the tumor.

Neoadjuvant treatment group

A total of 147 target LNs received neoCRT, including 102 in the training and 45 in the validation cohort. As shown in Table 5, in both cohorts, the short-diameter of positive LNs was significantly greater than those of negative LNs ($P < 0.001$). The short diameter regression in the positive was greater than negative in the validation cohort ($P < 0.05$); there was no difference in the degree of regression. Morphologically, border contour, internal signal, and signal intensity

were statistically different between the positive and negative LNs ($P < 0.05$). When the short diameter was 5.15–5.25 mm, the AUC was 0.838 (95% CI, 0.758–0.918) and 0.912 (95% CI, 0.825–0.999) in the training and validation cohorts. The corresponding ROC curves and AUC values are shown in Fig. 8 and Table 3. The median short-axis diameter after neoadjuvant therapy was 3.8 mm (range: 2.5–9.0 mm) and 6.2 mm (range: 3.2–12.2 mm) for the negative and positive nodules, respectively. The histogram of LN distribution under different short diameters is shown in Fig. 9.

The results of the multivariate analysis are shown in Table 6. The short diameter, border contour, internal signal, signal intensity, ymrT-stage, MRI-EMVI, MRI-CRM, and tumor diameter were chosen from the training cohort as covariates for logistic regression analysis. Multivariate

Table 3 Predictive efficacy of short diameter and nomogram in the primary surgery group and neoadjuvant therapy group

	Cohorts	Model	AUC (95%CI)	Cut-off	Sensitivity	Specificity	PPV	NPV
PS group	Training	Short diameter	0.661 (0.520–0.802)	5.250	0.565	0.835	0.260	0.949
		Nomogram	0.855 (0.794–0.916)	0.087	0.870	0.732	0.250	0.982
	Validation	Short diameter	0.749 (0.562–0.936)	5.500	0.600	0.896	0.375	0.956
		Nomogram	0.854 (0.727–0.980)	0.098	0.800	0.844	0.348	0.976
NT group	Training	Short diameter	0.838 (0.758–0.918)	5.150	0.621	0.904	0.720	0.857
		Nomogram	0.912 (0.856–0.968)	0.290	0.828	0.890	0.750	0.929
	Validation	Short diameter	0.912 (0.825–0.999)	5.250	0.769	0.938	0.833	0.909
		Nomogram	0.915 (0.817–1.000)	0.286	0.846	0.906	0.786	0.935

PS primary surgery, *NT* neoadjuvant therapy, *AUC* area under the curve, *CI* confidence interval, *PPV* positive predict value, *NPV* negative predict value
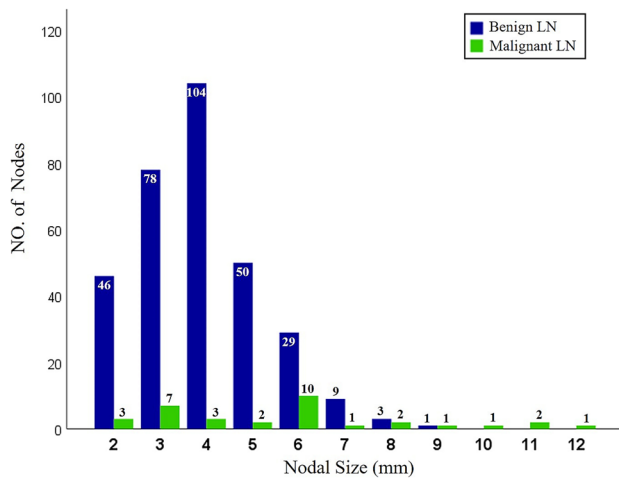
Fig. 4 The histogram of LN distribution under different short diameters in primary surgery group

logistic regression results demonstrated that the short diameter, ymrT-stage, internal signal, and MRI-EMVI were independent predictors of LNM ($p < 0.05$). A nomogram with 4 significant predictors is presented in Fig. 10. In the training cohort, the AUC of the nomogram was 0.912 (95% CI, 0.856–0.968), Hosmer Lemeshow goodness of fit test $p = 0.209$. The C-index was 0.892 and was confirmed to be 0.878 via 1000 bootstrapping validation. The AUC of the nomogram was shown to be 0.915 (95% CI, 0.817–1.000) in the validation cohort (Fig. 8 and Table 3). The nomogram had a bootstrapped-concordance index of 0.848 and was well calibrated (Fig. 11). In terms of distribution, 100% (42/42) of positive LNs were visualized at the level of the tumor or within 5 cm proximal to the tumor. (Fig. 12).

Discussion

Accurate assessment of mesorectal LN status has always been a critical concern, especially since neoadjuvant therapy plus total mesenteric excision (TME) has become the standard treatment for LARC. This study combined preoperative clinical and imaging biomarkers to construct nomograms based on mesorectal LN pathology-imaging matching and revealed that it could improve the prediction of nodal involvement.

Initial LN status is an important indication and prognostic factor for CRT. Evaluation based on MRI morphological criteria is still the most controversial issue in the preoperative staging of rectal cancer. A recent meta-analysis showed that, based on a node-by-node comparison, the sensitivity of MRI in identifying metastatic LNs was 0.40–0.69, and the specificity was 0.79–0.95 [21]. In this study, the short diameter of 5.25 mm obtained the highest accuracy in the training cohort, with moderate sensitivity and specificity (0.565 and 0.835) for detecting lymph node metastasis, close to the results of previous studies. However, thus far, there is still no consensus on the optimal cutoff value for LNM. Most studies choose 5–10 mm as the standard, and as the short diameter increases, the sensitivity gradually decreases and the specificity gradually increases [22–24]. Besides the size, the morphological features of LNs on T2WI were considered the more important criteria. Brown et al. first described that border and signal intensity improved the prediction of nodal involvement with 85% sensitivity and 97% specificity [7]. In our study, multivariate logistic regression analysis proved in this view that both border contour and signal intensity were independent predictors. Traditionally, metastatic LNs often appear with a sharp border on imaging, whereas

Table 4 Risk factors for lymph node metastasis in the primary surgery group

|				
mrT-stage	5.996 (2.292–15.688)	0.001	7.310 (1.647–32.442)	0.009
Shape				
Round	Reference	0.009		
Ovid	0.568 (0.198–1.630)	0.293		
Other	2.024 (0.754–5.435)	0.162		
Border contour				
Smooth	Reference	0.001	Reference	0.002
Lobulated	4.982 (1.054–23.552)	0.043	2.673 (0.482–14.811)	0.260
Spiculated	24.474 (5.355–111.844)	0.001	13.689 (2.445–76.652)	0.003
Indistinct	9.435 (1.891–47.082)	0.006	16.037 (2.676–96.112)	0.002
Internal signal	4.038 (1.888–8.636)	0.001		
Signal intensity				
Low	Reference	0.021	Reference	0.009
Iso	0.344 (0.158–0.749)	0.007	0.265 (0.097–0.727)	0.010
High	0.951 (0.293–3.086)	0.933	1.928 (0.402–9.257)	0.412

OR odds ratio, *CI* confidence interval
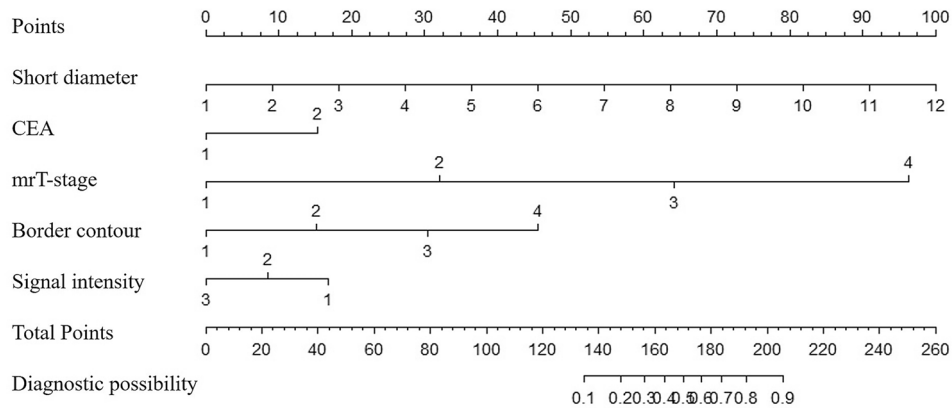
Fig. 5 Nomogram for predicting lymph node status in primary surgery-group, with 5 significant predictors including short diameter, preoperative CEA level, mrT-stage, border contour, and signal intensity. For short diameters, the number represents the short diameter value. For CEA, 1 means CEA levels within 0–5 (ng·mL^{-1}), and 2 means CEA levels are greater than 5 (ng·mL^{-1}). For mrT-stage, 1 represents mrT1-stage, 2 represents mrT2-stage, 3 represents mrT3-stage, and 4 represents mrT4-stage. For border contour, 1 represents border smooth, 2 represents border lobulated, 3 represents border spiculated, and 4 represents border indistinct. For signal intensity, 3 represents a high signal, 2 represents an iso signal, and 1 represents a low signal. From each variable location on the corresponding axis, a line was drawn straight upward to the point axis and a score was obtained. By summing the scores of each point and locating them on the total score scale, the estimated probability of lymph node metastases could be determined

inflammatory LNs have an indistinct margin. A desmoplastic reaction or tumor infiltration could cause this indistinct margin. Schnall et al. suggested that low LN signal intensity might predict tumor involvement, which was also confirmed by our findings [25]. After adding morphological criteria, our results indicate higher sensitivity but lower specificity. Since morphological criteria are difficult to obtain in small nodes, the diagnostic accuracy variation may be caused partly by difficulties and differences in interpreting nodal

features. In multivariate analysis, we observed that the mrT-stage and the average level of serum CEA were significantly associated with LNM ($p < 0.05$). T classification is an index of the depth of tumor, which is a definite cause of rectal cancer recurrence and metastasis [26, 27]. mrT-stage has been shown to have comparable accuracy in determining depth of tumor invasion [22, 24, 28]. CEA is the most common tumor marker of colorectal cancer. Preoperative serum CEA levels can reflect cancer status. A previous study revealed
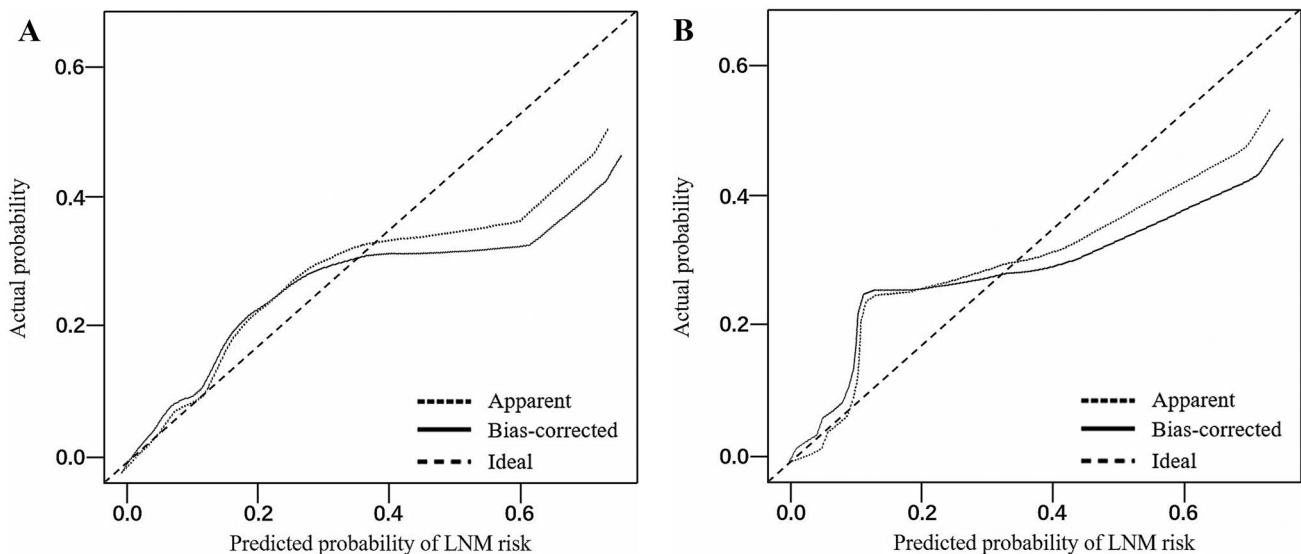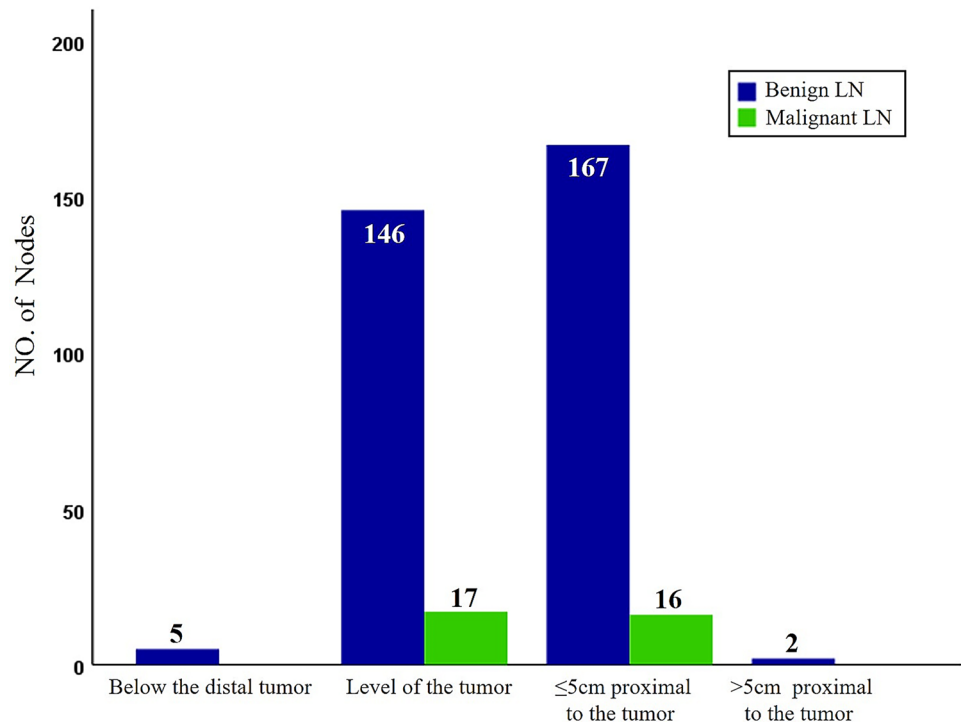

Fig. 6 Calibration curve of the nomogram in primary surgery-group. LNM, lymph node metastasis. **A** Calibration curve of the nomogram in the training cohort. **B** Calibration curve of the nomogram in the validation cohort

Fig. 7 The cranial-caudal distribution of the LN with the distal tumor margin in primary surgery-group

that elevated CEA was strongly correlated with LNM [29]. The model proposed by Xu H et al., including clinical T stage, N stage, CRM, EMVI, and CEA, had a sensitivity and specificity of 0.854 and 0.847 for predicting LNM of rectal cancer [30]. The corresponding values in the validation cohort predicted by the nomogram were 0.818 and 0.809, showing good prediction performance.

Researchers have shown that CRT can relieve some metastatic LNs but is unable to control all [31, 32]. Unresectable LNM can lead to local recurrence or distant metastasis, making clinical decision-making difficult. Currently, predicting LN status after CRT remains challenging, which can cause changes in LN morphology, size, number, and texture. Nevertheless, several studies have indicated that size criteria work better in restaging because LNs are shrunk and smaller due to irradiation. Thus, LNs that remained large after CRT were more likely to be malignant [33–35]. However, due to the difficulties in detecting and evaluating small nodes, the accuracy of MRI for nodal restaging ranges from 67 to 90% [36–39]. In our study, the 5.1 mm size cutoff obtained a much higher AUC than the primary surgery group, with a size cutoff lower than that of the initial stage. The established nomogram showed that the node size was included with a relatively high weight, which means that LNs with larger short diameters are more likely to metastasize. Therefore, size is more effective than size cutoffs when determining LN status after neoadjuvant therapy. In most current studies, the sensitivity was based only on the short diameter. Koh et al. assessed 152 LNs after neoadjuvant

therapy and obtained 67% sensitivity and 95% specificity by morphological criteria [34]. In the former prediction model, LN status is the interpretation of border and signal intensity. Indeed, we found that although morphological features were associated with LNM, only the internal signal was shown to be an independent predictor in multivariate analysis. One potential underlying cause of this finding: After establishing a node-by-node correlation, radiation-induced changes in the rectal wall and LNs after CRT may limit radiologists' accurate assessment of morphological features compared with initial staging; therefore, the morphological differences between benign and malignant LNs in restaging may be overestimated.

By assessing the correlation between clinical biomarkers and LNM, we found that MRI-EMVI is an independent predictor of restaging. MRI-EMVI refers to the specific features of the mesorectum examined by MRI, which was first proposed by Smith et al. [40]. Liu et al. reported that MRI-EMVI was associated with LN involvement and had an independent predictive ability for LNM [41]. In the validation cohort, the nomogram prediction model obtained an area under the curve of 0.915, corroborating previous findings.

Previous studies pointed out that the degree of regression was significantly correlated with the disappearance of LNM. When a node shows a remarkable decrease in size, it is highly likely that the node is benign [32]. Indeed, in our study, there was no difference between the two cohorts in residual LNs; those who decreased more than 1/2 still had a 9.5% (4/42) metastasis rate. The reason accounting for

Table 5 Lymph node characteristics in training and validation cohort in the neoadjuvant therapy group

Feature	Training cohort ($n=102$)		P-value	Validation cohort ($n=45$)		P-value
	Malignant LN ($n=29$)	Benign LN ($n=73$)		Malignant LN ($n=13$)	Benign LN ($n=32$)	
Short diameter (mm)	5.80 (3.2–11.3)	3.81 (2.5–8.1)	0.001**	7.06 (3.6–12.2)	3.79 (2.5–9.0)	0.001**
Short diameter regression (mm)	1.90 (0–8.7)	1.35 (0.1–5.4)	0.079**	2.00 (0.6–5.3)	1.20 (0.1–4.0)	0.035**
Degree of regression	0.23 ± 0.15	0.23 ± 0.18	0.948**	0.24 ± 0.12	0.23 ± 0.15	0.719**
Degree of regression group			0.520*			0.561*
≤ 1/4	20	42		9	19	
1/4 < and ≤ 1/2	6	23		3	12	
> 1/2	3	8		1	1	
Shape			0.287*			0.134*
Round	6	15		2	9	
Ovid	12	41		6	19	
Other	11	17		5	4	
Border contour			0.001*			0.001*
Smooth	0	25		0	8	
Lobulated	7	15		4	9	
Spiculated	20	21		8	3	
Indistinct	2	12		1	12	
Internal signal			0.001*			0.001*
Homogeneity	9	54		3	25	
Heterogeneity	20	19		10	7	
Signal			0.052*			0.648*
Low	18	31		8	17	
Iso	10	26		4	9	
High	1	16		1	6	
Distribution			0.840*			0.481*
Below the distal tumor	0	1		0	2	
Level of the tumor	14	33		4	13	
≤ 5 cm proximal to the tumor	15	38		9	17	
> 5 cm proximal to the tumor	0	1		0	0	

LN lymph node

* chi-square test; ** rank-sum test

this finding is that we excluded nodes that disappeared on post-CRT MRI because we could not clarify their pathology, in fact, nodes that are not visible anymore at post-CRT MRI have a meager chance of metastasis. Loftås et al. found the size of the largest LN after neoadjuvant therapy indicates node positivity. In that study, LNs of 8 mm or more in diameter were similarly correlated with ypN+ [42]. In our research, even though the positive rate above 8 mm reached 77%, there was still a high transfer rate between 4 and 10 mm. Conversely, only 12 of the 94 LNs with 5 mm or less diameter were metastatic (12.8%), which is different from Perez et al., who reported that 50% of metastatic LNs were smaller than 3 mm after CRT [33]. This may relate to the former only selected subgroup of ypT0-2 patients with significantly smaller LNs for retrospective analysis, while

the sensitivity of LNs to CRT is not the same. The proportion of complete remission (including complete fibrosis and mucus lake) in the mesorectal LNs after neoadjuvant therapy is 13.5–50%, as reported in the previous literature [43, 44]. This means the accuracy of current method assessments may be quite limited, especially in the setting of neoadjuvant therapy.

From the cranial-caudal distribution of the LNs, the most common locations are still at the level of the tumor or within 5 cm proximal to the tumor; the number of positive LNs in these two regions accounts for more than 95% of the total. This is primarily related to the dominant lymphatic drainage pathways associated with rectal cancer, with LNs draining upward within the mesorectum being a widely accepted theory. In our cohorts, all positive LNs were distributed within
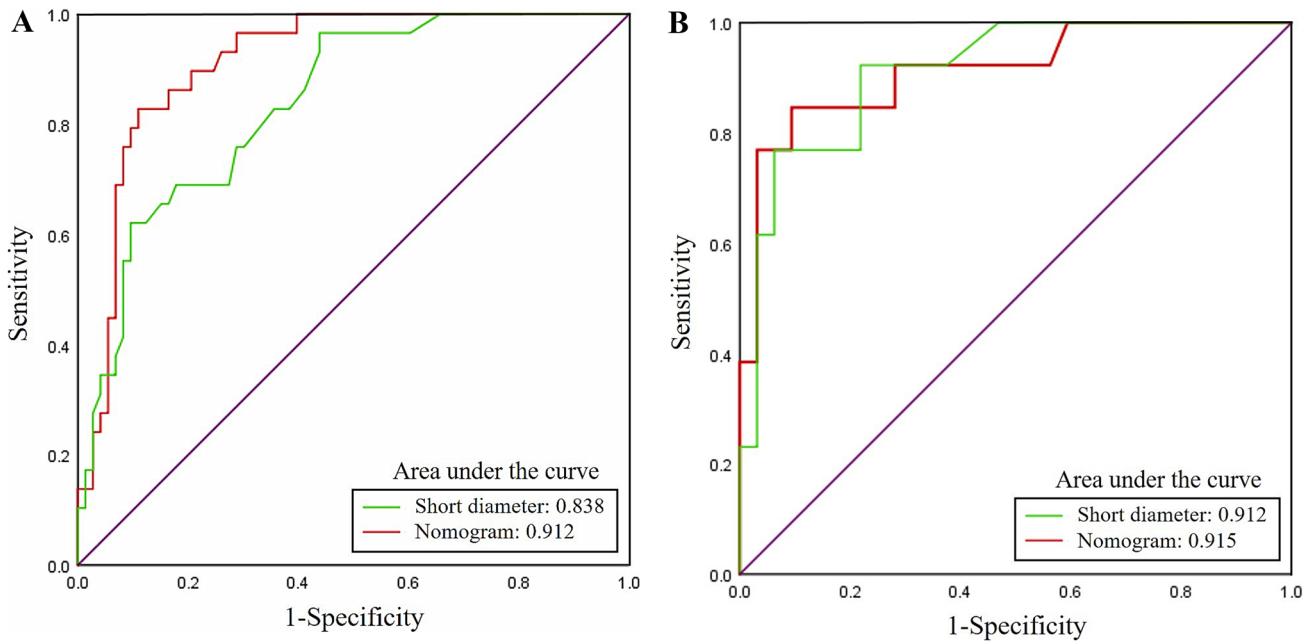
Fig. 8 Receiver operating characteristic (ROC) curve and prediction model based on short diameter and nomogram in neoadjuvant therapy group. **A** ROC curve in the training cohort. **B** ROC curve in the validation cohort

the horizontal or 5 cm proximal to the tumor, which is in line with other studies [12, 45].

To the best of our knowledge, this is the first prospective study to construct nomograms of preoperative clinical and imaging biomarkers based on mesorectal LN

pathology-imaging matching to improve the diagnostic accuracy of preoperative N staging and restaging and internally validated in the validation cohorts. Compared with obtaining staging results from all LNs, the pathological basis of a single LN is more convincing and can more accurately assess

Fig. 9 The histogram of LN distribution under different short diameters in neoadjuvant therapy-group
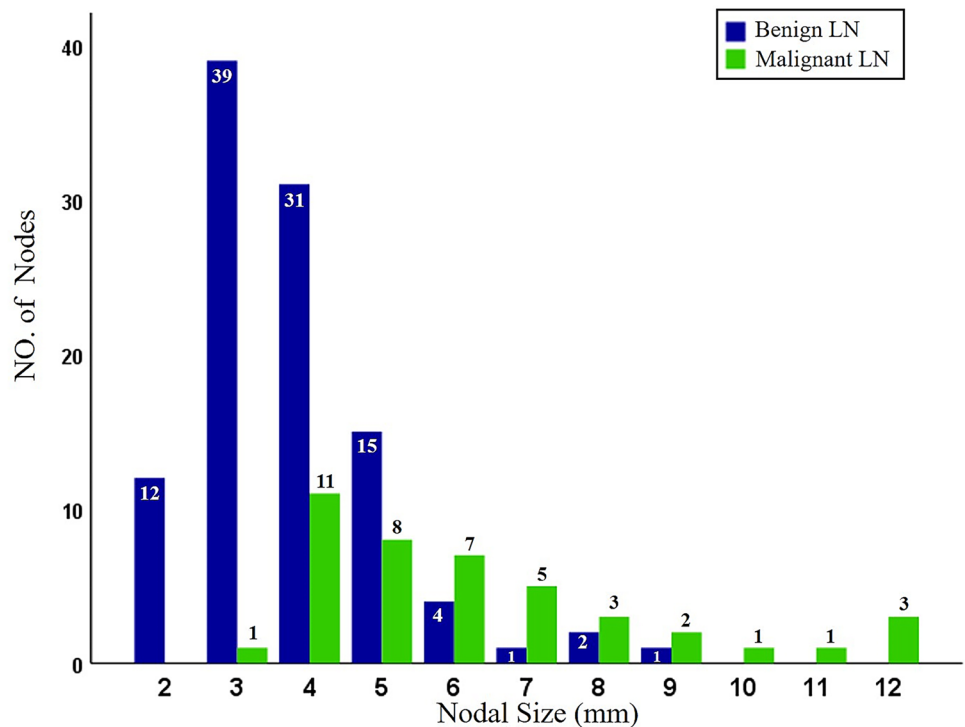
Table 6 Risk factors for lymph node metastasis in the neoadjuvant therapy group

Factors	Univariate logistic regression		Multivariate logistic regression	
	OR (95% CI)	P-value	OR (95% CI)	P-value
Short diameter	2.348 (1.699–3.246)	0.001	1.816 (1.291–2.554)	0.001
Tumor diameter	1.045 (1.019–1.072)	0.001		
MRI-CRM	0.400 (0.191–0.837)	0.015		
MRI-EMVI	0.292 (0.135–0.628)	0.002	0.277 (0.088–0.873)	0.048
ymrT-stage	3.945 (1.677–9.283)	0.002	0.080 (0.007–0.912)	0.042
Border contour	1.534 (1.063–2.213)	0.022		
Internal signal	7.596 (3.404–16.954)	0.001	3.602 (1.301–9.974)	0.014
Signal intensity	0.521 (0.302–0.900)	0.019		

OR odds ratio, *CI* confidence interval

the diagnostic value of nodal involvement. Although some studies have evaluated and established nomograms for predicting LNM, most risk factors include postoperative pathological features [46–48]. Indeed, compared with obtaining pathological results from surgical specimens, preoperative clinical and imaging features can be used as a more convenient method for individualized preoperative assessment. Due to the limitation of spatial resolution, current imaging methods cannot accurately identify LNs smaller than 2 mm. This also explains the higher matching success rate of 93.9% (500/532), but a large discrepancy between the number of LNs identified by histopathology 500/1337 (37%). Among the unmatched LNs, the incidence of malignancy was 36/877 (4.1%), indicating that the matching process can include most malignant nodes. Since 2010, several new techniques for improving N-staging have been published, using a variety of LN involvement diagnostic criteria and markers

including lymph node contrast agents, radiomic models, specific MRI parameters, etc. has shown some success [18–20, 31, 49]. Nevertheless, given these technical price costs, the time-consuming calculation process and practicality make it challenging to achieve clinical translation in the short term. In this way, the current dimensional criterion remains the most widely used because it is the simplest and readily available in clinical practice.

This study has some limitations. First, the present study lacked external validation. Second, despite the relatively high total number of anatomically matched LNs in staging or restaging, the number of malignant LNs was small. Third, despite matching all histologically found LNs as far as possible, the number of LNs within different short-axis diameters varies widely, especially for nodes smaller than 2 mm. This limitation highlights the ongoing challenge of accurately describing mesorectal LNs.
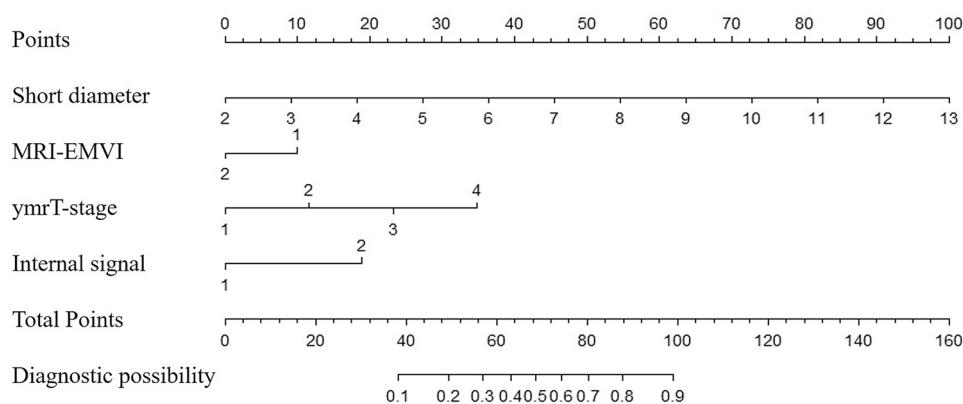

Fig. 10 Nomogram for predicting lymph node status in neoadjuvant therapy-group, with 4 significant predictors including short diameter, MRI-EMVI, ymrT-stage, and internal signal. For short diameters, the number represents the short diameter value. For MRI-EMVI, 2 means MRI-EMVI negative, and 1 means MRI-EMVI positive. For ymrT-stage, 1 represents ymrT1-stage, 2 represents ymrT2-stage, 3 represents ymrT3-stage, and 4 represents ymrT4-stage. For internal signals, 1 stands for signal homogeneity and 2 for signal heterogeneity. From each variable location on the corresponding axis, a line was drawn straight upward to the point axis and a score was obtained. By summing the scores of each point and locating them on the total score scale, the estimated probability of lymph node metastases could be determined
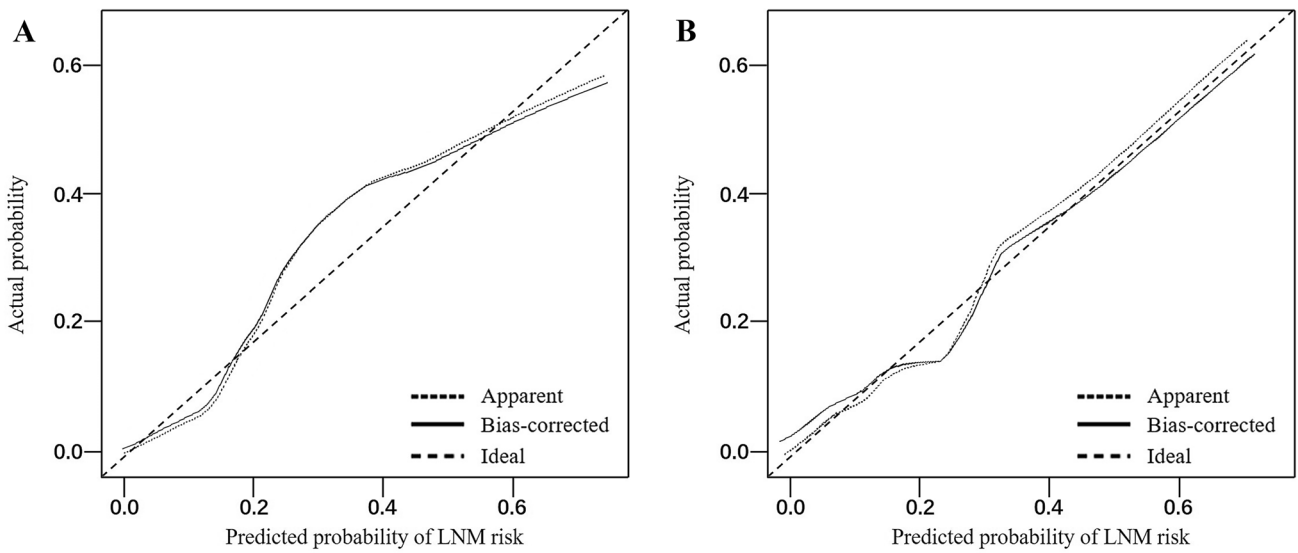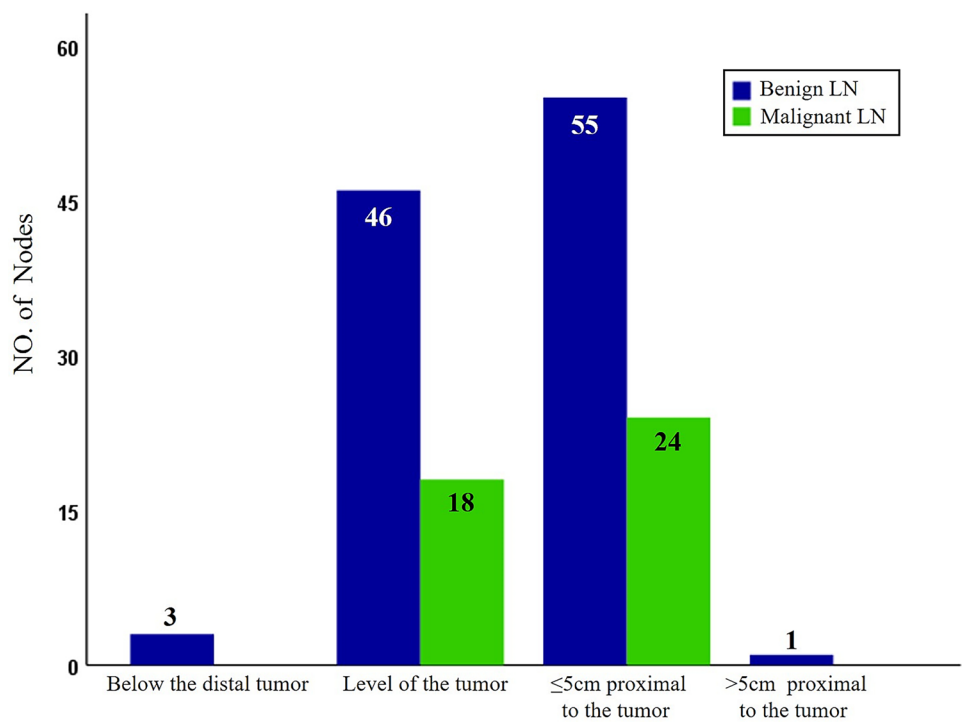
Fig. 11 Calibration curve of the nomogram in neoadjuvant therapy-group. LNM, lymph node metastasis. **A** Calibration curve of the nomogram in the training cohort. **B** Calibration curve of the nomogram in the validation cohort

Fig. 12 The cranial-caudal distribution of the LN with the distal tumor margin in neoadjuvant therapy-group

Conclusion

In conclusion, this study presents nomograms incorporating preoperative clinical and imaging biomarkers, which will aid in selecting a significant proportion of patients for alternative treatment strategies at staging and restaging. However, these results should be interpreted with caution because more extensive prospective studies are needed to validate the diagnostic performance of nomograms.

Declarations

Ethics approval This study was approved by the Medical Ethics Committee of West China Hospital.

Consent to participate Informed consent was obtained from all individual participants included in the study.

Competing interests The authors declare no competing interests.

References

1. Siegel RL, Miller KD, Goding Sauer A, Fedewa SA et al (2020) Colorectal cancer statistics, 2020. CA Cancer J Clin 70(3):145–164. https://doi.org/10.3322/caac.21601
2. Wiegering A, Isbert C, Dietz UA, Kunzmann V et al (2014) Multimodal therapy in treatment of rectal cancer is associated with improved survival and reduced local recurrence - a retrospective analysis over two decades. BMC Cancer 6(14):816. https://doi.org/10.1186/1471-2407-14-816
3. Benson AB, Venook AP, Al-Hawary MM, Arain MA et al (2020) NCCN guidelines insights: rectal cancer, Version 6.2020. J Natl Compr Canc Netw 18(7):806–815. https://doi.org/10.6004/jnccn.2020.0032
4. Glynne-Jones R, Wyrwicz L, Tiret E, Brown G, ESMO Guidelines Committee et al (2017) Rectal cancer: ESMO clinical practice guidelines for diagnosis, treatment and follow-up. Ann Oncol 28(4):22–40. https://doi.org/10.1093/annonc/mdx224
5. Bipat S, Glas AS, Slors FJ, Zwinderman AH et al (2004) Rectal cancer: local staging and assessment of lymph node involvement with endoluminal US, CT, and MR imaging–a meta-analysis. Radiology 232(3):773–783. https://doi.org/10.1148/radiol.2323031368
6. Li XT, Sun YS, Tang L, Cao K, Zhang XY (2015) Evaluating local lymph node metastasis with magnetic resonance imaging, endoluminal ultrasound and computed tomography in rectal cancer: a meta-analysis. Colorectal Dis 17(6):O129–O135. https://doi.org/10.1111/codi.12909
7. Brown G, Richards CJ, Bourne MW, Newcombe RG et al (2003) Morphologic predictors of lymph node status in rectal cancer with use of high-spatial-resolution MR imaging with histopathologic comparison. Radiology 227(2):371–377. https://doi.org/10.1148/radiol.2272011747
8. Kim JH, Beets GL, Kim MJ, Kessels AG, Beets-Tan RG (2004) High-resolution MR imaging for nodal staging in rectal cancer: are there any criteria in addition to the size? Eur J Radiol 52(1):78–83. https://doi.org/10.1016/j.ejrad.2003.12.005
9. Koh DM, Brown G, Temple L, Raja A et al (2004) Rectal cancer: mesorectal lymph nodes at MR imaging with USPIO versus histopathologic findings–initial observations. Radiology 231(1):91–99. https://doi.org/10.1148/radiol.2311030142
10. Park JS, Jang YJ, Choi GS, Park SY et al (2014) Accuracy of preoperative MRI in predicting pathology stage in rectal cancers: node-for-node matched histopathology validation of MRI features. Dis Colon Rectum 57(1):32–38. https://doi.org/10.1097/DCR.0000000000000004
11. Rutegård MK, Båtsman M, Blomqvist L, Rutegård M et al (2020) Rectal cancer: a methodological approach to matching PET/MRI to histopathology. Cancer Imaging 20(1):80. https://doi.org/10.1186/s40644-020-00347-6
12. Koh DM, Brown G, Temple L, Blake H et al (2005) Distribution of mesorectal lymph nodes in rectal cancer: in vivo MR imaging compared with histopathological examination. Initial observations. Eur Radiol 15(8):1650–1657. https://doi.org/10.1007/s00330-005-2751-8
13. Okada K, Sadahiro S, Suzuki T, Tanaka A et al (2014) Effects of chemoradiotherapy on lymph nodes in patients with rectal adenocarcinoma: evaluation of numbers and sizes of retrieved lymph nodes inside and outside the radiation field. Anticancer Res 34(8):4195–4200
14. Marijnen CA (2015) Organ preservation in rectal cancer: have all questions been answered? Lancet Oncol 16(1):e13-22. https://doi.org/10.1016/S1470-2045(14)70398-5
15. Chen CC, Lee RC, Lin JK, Wang LW, Yang SH (2005) How accurate is magnetic resonance imaging in restaging rectal cancer in patients receiving preoperative combined chemoradiotherapy? Dis Colon Rectum 48(4):722–728. https://doi.org/10.1007/s10350-004-0851-1
16. Mou S, Soetikno R, Shimoda T, Rouse R, Kaltenbach T (2013) Pathologic predictive factors for lymph node metastasis in submucosal invasive (T1) colorectal cancer: a systematic review and meta-analysis. Surg Endosc 27(8):2692–2703. https://doi.org/10.1007/s00464-013-2835-5
17. Glasgow SC, Bleier JI, Burgart LJ, Finne CO, Lowry AC (2012) Meta-analysis of histopathological features of primary colorectal cancers that predict lymph node metastases. J Gastrointest Surg 16(5):1019–1028. https://doi.org/10.1007/s11605-012-1827-4
18. Lahaye MJ, Engelen SM, Kessels AG, de Bruïne AP et al (2008) USPIO-enhanced MR imaging for nodal staging in patients with primary rectal cancer: predictive criteria. Radiology 246(3):804–811. https://doi.org/10.1148/radiol.2463070221
19. Lambregts DM, Beets GL, Maas M, Kessels AG et al (2011) Accuracy of gadofosveset-enhanced MRI for nodal staging and restaging in rectal cancer. Ann Surg 253(3):539–545. https://doi.org/10.1097/SLA.0b013e31820b01f1
20. Zhang H, Zhang C, Zheng Z, Ye F et al (2017) Chemical shift effect predicting lymph node status in rectal cancer using high-resolution MR imaging with node-for-node matched histopathological validation. Eur Radiol 27(9):3845–3855. https://doi.org/10.1007/s00330-017-4738-7
21. Zhuang Z, Zhang Y, Wei M, Yang X, Wang Z (2021) Magnetic resonance imaging evaluation of the accuracy of various lymph node staging criteria in rectal cancer: a systematic review and meta-analysis. Front Oncol 13(11):709070. https://doi.org/10.3389/fonc.2021.709070
22. Curvo-Semedo L (2020) Rectal cancer: staging. Magn Reson Imaging Clin N Am 28(1):105–115. https://doi.org/10.1016/j.mric.2019.09.003

23. Akasu T, Iinuma G, Takawa M, Yamamoto S et al (2009) Accuracy of high-resolution magnetic resonance imaging in preoperative staging of rectal cancer. Ann Surg Oncol 16(10):2787–2794. https://doi.org/10.1245/s10434-009-0613-3

24. Koh DM, Brown G, Husband JE (2006) Nodal staging in rectal cancer. Abdom Imaging 31(6):652–659. https://doi.org/10.1007/s00261-006-9021-3

25. Schnall MD, Furth EE, Rosato EF, Kressel HY (1994) Rectal tumor stage: correlation of endorectal MR imaging and pathologic findings. Radiology 190(3):709–714. https://doi.org/10.1148/radiology.190.3.8115616

26. Resch A, Langner C (2015) Risk assessment in early colorectal cancer: histological and molecular markers. Dig Dis 33(1):77–85. https://doi.org/10.1159/000366036

27. Sitzler PJ, Seow-Choen F, Ho YH, Leong AP (1997) Lymph node involvement and tumor depth in rectal cancers: an analysis of 805 patients. Dis Colon Rectum 40(12):1472–1476. https://doi.org/10.1007/BF02070714

28. Kim NK, Kim MJ, Park JK, Park SI, Min JS (2000) Preoperative staging of rectal cancer with MRI: accuracy and clinical usefulness. Ann Surg Oncol 7(10):732–737. https://doi.org/10.1007/s10434-000-0732-3

29. Nozoe T, Rikimaru T, Mori E, Okuyama T, Takahashi I (2006) Increase in both CEA and CA19–9 in sera is an independent prognostic indicator in colorectal carcinoma. J Surg Oncol 94(2):132–137. https://doi.org/10.1002/jso.20577

30. Xu H, Zhao W, Guo W, Cao S et al (2021) Prediction model combining clinical and MR data for diagnosis of lymph node metastasis in patients with rectal cancer. J Magn Reson Imaging 53(3):874–883. https://doi.org/10.1002/jmri.27369

31. Zhou X, Yi Y, Liu Z, Zhou Z et al (2020) Radiomics-based preoperative prediction of lymph node status following neoadjuvant therapy in locally advanced rectal cancer. Front Oncol 11(10):604. https://doi.org/10.3389/fonc.2020.00604

32. Heijnen LA, Maas M, Beets-Tan RG, Berkhof M et al (2016) Nodal staging in rectal cancer: why is restaging after chemoradiation more accurate than primary nodal staging? Int J Colorectal Dis 31(6):1157–1162. https://doi.org/10.1007/s00384-016-2576-8

33. Perez RO, Pereira DD, Proscurshim I, Gama-Rodrigues J et al (2009) Lymph node size in rectal cancer following neoadjuvant chemoradiation–can we rely on radiologic nodal staging after chemoradiation? Dis Colon Rectum 52(7):1278–1284. https://doi.org/10.1007/DCR.0b013e3181a0af4b

34. Koh DM, Chau I, Tait D, Wotherspoon A et al (2008) Evaluating mesorectal lymph nodes in rectal cancer before and after neoadjuvant chemoradiation using thin-section T2-weighted magnetic resonance imaging. Int J Radiat Oncol Biol Phys 71(2):456–461. https://doi.org/10.1016/j.ijrobp.2007.10.016

35. Sprenger T, Rothe H, Becker H, Beissbarth T et al (2013) Lymph node metastases in rectal cancer after preoperative radiochemotherapy: impact of intramesorectal distribution and residual micrometastatic involvement. Am J Surg Pathol 37(8):1283–1289. https://doi.org/10.1097/PAS.0b013e3182886ced

36. Barbaro B, Fiorucci C, Tebala C, Valentini V et al (2009) Locally advanced rectal cancer: MR imaging in prediction of response after preoperative chemotherapy and radiation therapy. Radiology 250(3):730–739. https://doi.org/10.1148/radiol.2503080310

37. Lahaye MJ, Beets GL, Engelen SM, Kessels AG et al (2009) Locally advanced rectal cancer: MR imaging for restaging after neoadjuvant radiation therapy with concomitant chemotherapy. Part II. What are the criteria to predict involved lymph nodes? Radiology 252(1):81–91. https://doi.org/10.1148/radiol.2521081364

38. Pomerri F, Pucciarelli S, Maretto I, Zandonà M et al (2011) Prospective assessment of imaging after preoperative chemoradiotherapy for rectal cancer. Surgery 149(1):56–64. https://doi.org/10.1016/j.surg.2010.03.025

39. van der Paardt MP, Zagers MB, Beets-Tan RG, Stoker J, Bipat S (2013) Patients who undergo preoperative chemoradiotherapy for locally advanced rectal cancer restaged by using diagnostic MR imaging: a systematic review and meta-analysis. Radiology 269(1):101–112. https://doi.org/10.1148/radiol.13122833

40. Smith NJ, Barbachano Y, Norman AR, Swift RI et al (2008) Prognostic significance of magnetic resonance imaging-detected extramural vascular invasion in rectal cancer. Br J Surg 95(2):229–236. https://doi.org/10.1002/bjs.5917

41. Liu L, Liu M, Yang Z, He W et al (2016) Correlation of MRI-detected extramural vascular invasion with regional lymph node metastasis in rectal cancer. Clin Imaging 40(3):456–460. https://doi.org/10.1016/j.clinimag.2016.01.007

42. Loftås P, Sturludóttir M, Hallböök O, Almlöv K et al (2018) Assessment of remaining tumour involved lymph nodes with MRI in patients with complete luminal response after neoadjuvant treatment of rectal cancer. Br J Radiol 91(1087):20170938. https://doi.org/10.1259/bjr.20170938

43. Caricato M, Ausania F, De Dominicis E, Vincenzi B et al (2007) Tumor regression in mesorectal lymphnodes after neoadjuvant chemoradiation for rectal cancer. Eur J Surg Oncol 33(6):724–728. https://doi.org/10.1016/j.ejso.2007.01.023

44. Li J, Yuan J, Liu H, Yin J et al (2016) Lymph nodes regression grade is a predictive marker for rectal cancer after neoadjuvant therapy and radical surgery. Oncotarget 7(13):16975–16984. https://doi.org/10.18632/oncotarget.7703

45. Heijnen LA, Lambregts DM, Lahaye MJ, Martens MH et al (2016) Good and complete responding locally advanced rectal tumors after chemoradiotherapy: where are the residual positive nodes located on restaging MRI? Abdom Radiol (NY) 41(7):1245–1252. https://doi.org/10.1007/s00261-016-0640-z

46. Zhou C, Liu HS, Liu XH, Zheng XB et al (2019) Preoperative assessment of lymph node metastasis in clinically node-negative rectal cancer patients based on a nomogram consisting of five clinical factors. Ann Transl Med 7(20):543. https://doi.org/10.21037/atm.2019.09.127

47. Huang YQ, Liang CH, He L, Tian J et al (2016) Development and validation of a radiomics nomogram for preoperative prediction of lymph node metastasis in colorectal cancer. J Clin Oncol 34(18):2157–2164. https://doi.org/10.1200/JCO.2015.65.9128

48. Liu Y, Wan L, Peng W, Zou S et al (2021) A magnetic resonance imaging (MRI)-based nomogram for predicting lymph node metastasis in rectal cancer: a node-for-node comparative study of MRI and histopathology. Quant Imaging Med Surg 11(6):2586–2597. https://doi.org/10.21037/qims-20-1049

49. Liu X, Yang Q, Zhang C, Sun J et al (2021) Multiregional-based magnetic resonance imaging radiomics combined with clinical data improves efficacy in predicting lymph node metastasis of rectal cancer. Front Oncol 18(10):585767. https://doi.org/10.3389/fonc.2020.585767